Title Page

Drastic Change of Local Stiffness Distribution Correlating to Cell Migration in Living Fibroblasts

Masafumi Nagayama*, Hisashi Haga and Kazushige Kawabata

Division of Physics, Graduate School of Science, Hokkaido University, Sapporo 060-0810, Japan

*To whom correspondence should be addressed.

Masafumi Nagayama, Division of Physics, Graduate School of Science, Hokkaido University, North 10, West 8, Kita-ku, Sapporo 060-0810, Japan

Tel: +81-11-706-2690

Fax: +81-11-706-4926

email: masafumi@skws.sci.hokudai.ac.jp

short running title: Drastic Change of Stiffness in Fibroblasts

ABSTRACT

Sequential images of the local stiffness distribution of living fibroblasts (NIH3T3) were captured under a culture condition using scanning probe microscopy in a force modulation mode. We found a clear relation between cell migration and local stiffness distribution on the cell: When cells were stationary at one position, the stiffness distribution of their cellular surface was quite stable. On the other hand, once the cells started to move, the stiffness in their nuclear regions drastically decreased. Possible explanations for the correlation between the cell migration and the cell stiffness are proposed.

Key words: scanning probe microscopy; force modulation mode; actin filaments; NIH3T3; cell movement

INTRODUCTION

Cell movement is one of the most fundamental functions, playing a role in phenomena raging from healing of wounded tissue to self-organizing of the early embryo. Such movement, also known as cell crawling, is considered to result from two major phenomena: elongation of leading edges at the anterior parts of a cell and contraction of posterior ones [for review see Horwitz and Parsons, 1999; Lauffenburger and Horwitz, 1996]. Dynamical rearrangement of the cytoskeleton is essential for both elongation and contraction. Numerous studies have also shown that Rho family of small GTPases including RhoA, Rac1, and Cdc42 is key regulator of the cytoskeletal dynamics. In addition to the cytoskeletal filaments and the Rho GTPases, integrin, extra cellular matrix, membrane and focal contact are also considered to contribute to the cell migration. However, it is not clearly understood how these various elements cooperate throughout the cell to induce cell crawling in a given direction.

Recently, mechanical properties of living cells have been focused to clarify the mechanism of such cooperative phenomena as the cell migration. A tensegrity model is known as a conceptual model on correlation between elasticity and dynamics of cytoskeletons [Ingber, 1993; Ingber, 1997]. Various methods have been proposed for measuring the elasticity of living cells, such as magnetic beads [Bausch et al., 1998; Bausch et al., 1999; Wang and Stamenovic, 2000], cell poking [Peterson et al., 1982;

Zaharak et al., 1990], scanning acoustic microscopy [Bereiter-Hahn et al., 1995; Hildebrand and Rugar, 1984; Lures et al., 1991], micropipette aspiration [Evans et al., 1995; Shao and Hochmuth, 1996], and optical tweezers [Ashkin and Dziedzic, 1989; Henon et al., 1999; Svoboba et al., 1992]. However, temporal and/or spatial resolution of these methods is not sufficiently high to discuss the mechanical properties with respect to cell migration.

Scanning probe microscopy (SPM) was developed as a powerful tool for measuring the mechanical properties of living cells on a nanometer scale and within a nano-Newton range [Radmacher et al., 1993; Radmacher et al., 1996]. We have reported that local elastic moduli are not uniform over the cellular surface of a living fibroblast but vary from several kPa to a few hundred kPa depending on the position of the cell [Haga et al., 2000a]. Immunofluorescence observations with chemical doping strongly suggest that the local elasticity is mainly attributed to actin filaments rather than microtubules [Kawabata et al., 2001; Rotsch and Radmacher, 2000; Walch et al., 2000; Wu et al., 1998]. Furthermore, our detailed comparison between the local stiffness and density of actin filaments of fibroblasts revealed that the local stiffness does not originate only from the actin filament density [Haga et al., 2000a].

In this study, we measured the time dependence of the local stiffness distribution of living fibroblasts to clarify the cooperative mechanism for cell migration. The measurements were carried out using the force modulation mode with SPM, which has

higher temporal and spatial resolution than the force mapping mode. Comparing the local stiffness distribution of the cells between moving and stationary states of the cell migration, we found a clear relation between cell migration and local stiffness distribution on the cell.

MATERIALS AND METHODS

Sample Preparation and SPM Imaging

Fibroblasts (NIH3T3) were used for the present measurements. The cells were purchased from RIKEN Cell Bank (Tsukuba, Japan), and cultured in low glucose Dulbecco's modified Eagle's medium (DMEM) containing 10% fetal bovine serum (GIBCO BRL, Basel, Switzerland). The cells grown in plastic flasks were maintained at 37°C and 5% CO_2 in a humidified incubator. The confluent cells were trypsinized and released from the plastic flasks. For the SPM imaging, the cell suspension was plated on a glass petri dish precoated with fibronectin (Boehringer Mannheim, Mannheim, Germany), and then incubated for at least one night. To keep constant pH during the SPM measurements, preheated HEPES-buffer (pH 7.2~7.3) was substituted for the culture medium, and the samples were incubated for 1 hour before the measurement.

A commercial instrument composed of an SPA400 and SPI3800 (Seiko Instruments Inc., Chiba, Japan) was used for the SPM measurements. The equipped piezo scanner had a maximal x-y scan range of 100 μm each direction and a z range of 10 μm. We used commercially available silicon-nitride cantilevers with an effective length of 220 μm and a pyramidal tip which typical radius of curvature is about 50 nm. (ThermoMicroscopes, Sunnyvale, CA). The typical spring constant of cantilevers was 0.03 N/m. Cell topographies were measured in the contact mode at a loading force of 2 nN, so that the

cellular surfaces were indented about 100 nm during the measurements. The topographic images were shaded using photo retouch software to render the morphology of the cellular surface more distinct. The temperature of the buffer solution was controlled at 33±0.5°C to maintain physiological conditions throughout the experiments. The cells adhered thinly and firmly to the substrate during and after the SPM experiments. This verified that the present experiments were performed under the physiological condition, and did not cause any damage to the cells.

Force Modulation Mode

Stiffness imaging was performed using the force modulation mode [Haga et al., 2000b; Radmacher et al., 1993]. This mode can estimate both elastic and viscous properties of samples by detecting the sample indentation caused by external stress. To load stress to the sample, sinusoidal vibration whose amplitude was about 10 nm was applied to the cantilever (or the piezo scanner) by using a function generator (AFG310; SONY, Tokyo, Japan) during the contact mode scanning. The periodical strain of the sample was detected as a cantilever deflection. The oscillating component of the cantilever deflection that reflects viscoelasticity of the sample was extracted through a two-phase lock-in amplifier (Model 5210; PAR, Oak Ridge, TN). Theoretically, frequency dependence of the viscoelasticity can be measured by varying the oscillating frequency. In the liquid environment, however, the oscillating frequency should be set as low as possible, because

the viscous influence surrounding the sample cannot be neglected at the higher frequency. On the other hand, at lower frequency, the temporal resolution becomes poorer. Thus, the oscillating frequency was set at 500 Hz, which frequency has a temporal resolution of 6 minutes for a 128 pixels x 64 lines image, and was not varied in the present work. At the frequency of 500 Hz, the feedback system for measuring topography can cancel the periodical stress applied by the cantilever vibration. To avoid this influence, a band elimination filter (3624; NF, Yokohama, Japan) was used to remove the oscillating component from the cantilever deflection signal sent to the feedback system [details of the instrumentation will be published in the near future].

The viscoelasticity of the sample was calculated from amplitude and phase data by the method based on the linear viscoelastic theory [Haga et al., 2000b]. The output signals from the two-phase lock-in amplifier represent the amplitude ratio β and phase lag θ_s of the cantilever deflection relative to the reference signals from the function generator. Using the experimental data β and θ_s, the Young's modulus E and viscous coefficient η of the sample can be expressed as

$$E = C_1 \frac{\beta(\cos\theta_S - \beta)}{1+\beta^2-2\beta\cos\theta_S}$$
$$\eta = C_2 \frac{\beta\sin\theta_S}{1+\beta^2-2\beta\cos\theta_S} \quad ,$$

where C_1 and C_2 are instrumental constants including the spring constant of the cantilever, etc. For purpose of simplicity, we assumed that C_1 and C_2 were equal to 1, so

that the values of E and η were qualitative ones.

The value of E is estimated from a mechanical response of samples against cantilever indentation. In the case of the mechanical response originating only from the elastic property of samples, E simply represents the Young's modulus of the materials. In the present case, however, the mechanical response from the cellular surface is expected to include many other mechanical effects, including the surface tension. Thus, in this study, E was designated as effective value of local stiffness rather than elastic modulus.

RESULTS

Figure 1 shows typical topographic, local stiffness and viscous images of a living fibroblast. The cell extends very thinly on the substrate and elongates toward the direction of crawling. Its height is about 3 μm. Many stress fibers appear on the cellular surface and align along the direction of movement. In the stiffness image, brighter areas represent greater hardness. We have confirmed that the distribution of the local stiffness measured by the force modulation mode is in good agreement with that obtained by the force mapping mode to the identical cell [Haga et al., 2000b]. Therefore, the stiffness distributions measured by the force modulation mode here would range from several kPa to a few hundred kPa. It was found that local stiffness is not homogeneous on the cellular surface but varies largely from point to point. The stress fibers seen in the topographic image are harder than the surroundings, and this finding was consistent with the previous results [Haga et al., 2000b; Kawabata et al., 2001; Rotsch and Radmacher, 2000]. In the viscous image, brighter areas represent higher viscosity. The local viscosity of the area of the nucleus (described by an oval in the figure 1c) appeared to be lower than that of the periphery. This result was also consistent with those reported previously [Haga et al., 2000b]. However, further detailed, quantitative analysis will still be needed, because the values of viscosity in the nano scale have never been compared with those by other methods. For this reason, we here discuss only the topography and stiffness of the cells.

Sequential sets of topographic and local stiffness images of a typical moving cell are shown in Fig. 2. The topographic and stiffness images were taken simultaneously. The images were captured every 10 minutes. The SPM measurements were continued for about 60 minutes, which corresponds to the average time period of the intermittent cell crawling. The cell is changing its shape and moving downward in the image. A part of the cell is contracting, and the lamellipodia is extending gradually during the measurement. Accompanying with the change in shape, the position of the nucleus (marked by a cross in each image) is moving downward in the time course of images (a) through (f). It should be noted that the local stiffness distribution also changes drastically with the cell migration. The area of the nucleus within the oval in images (a) and (b) is harder than the peripheral regions. Then, when the cell begins to move, this area becomes softer. This result indicates that the local stiffness distribution of the cell correlates to the cell migration. The same results were observed in three other cells without exception. Based on our previous result obtained by the force mapping mode, it can be estimated that the stiffness of nucleus region decreases form a hundred kPa to several kPa during migration [Haga et al., 2000b].

To verify this correlation, the time dependence of the local stiffness distribution of the cell was also measured in the case that the cell was staying at a position. Figure 3 shows the sequential sets of topographic and stiffness images of the cell over a period of 60 minutes. The cell does not change either its shape or its position during the measurement.

In the stiffness images, the stiffer stress fibers run across the entire cellular surface. In contrast with the results on the moving cells, the local stiffness distribution of the staying cell does not change temporally. This result indicates that the stiffness of the fibroblasts does not show any spontaneous periodic change, such as a cardiac cycle. The average values of the local stiffness on the nuclear areas in both the moving cell (Fig. 2) and staying cell (Fig. 3) are plotted as a function of time in Fig.4. When the cell begins to move, the stiffness of the nuclear area drastically decreased. In contrast, the stiffness of the staying cell is almost constant throughout this time period.

DISCUSSION

We propose two possible models to account for the correlation between the cell migration and the change in stiffness distribution.

In the first, tensional force acting along the stress fibers would have changed with the cell migration. The tensional force, which is caused mainly by interaction between actin filament and myosin-II, is known to act at focal contacts when the cells are crawling on the substrate [Dembo and Wang, 1999]. The tension acting along the stress fibers is expected to change according to the cell crawling. The local stiffness obtained by SPM was estimated from the mechanical response of samples to cantilever indentation. Then, the change of the tension along the stress fibers would have induced the change of local stiffness measured by SPM, and this induction would have been equivalent to that by the elasticity of the actin filament network. When the cells were moving, the tension along the stress fibers would increase and finally exceed the adhesive force between the stress fibers and the substrate at focal contacts. This would lead to detachment of the posterior portion of the cell from the substrate and initiation of cell migration. In this case, the local stiffness would increase before the detachment, and decrease just after initiation of the cell migration. Therefore, cells would migrate by repeating the periodic change of the stiffness.

The second model involves the change of elasticity of the actin filament network with

the cell migration. The actin filaments are cross-linked in different way by the associated proteins, such as filamin or finblin. These form cell cortex and stress fibers, which have characteristic network structures with different Young's modulus. The local stiffness measured by SPM can vary depending on the associated proteins, even if the density of actin filaments is identical [Maciver et al., 1991]. If the actin filament network under the cell membrane lost the rigid structures, the cell could become so deformable as to move. This could explain the drastic decrease of the local stiffness just after the initiation of the cell migration.

CONCLUSIONS

We measured the sequential images of the topography and the local stiffness distribution of living fibroblasts by SPM. We discovered a clear correlation between the change of the local stiffness distribution and the intermittent cell migration. Two possible mechanisms were proposed to explain this correlation: the tension acting on actin filaments or the actin network structures associated with the binding proteins. At this stage, it is difficult to decide which model is responsible for the cell migration. However, we prefer the tension model, since a large tension should act on the cells as driving force inducing the migration. The result that highly spread cells are stiffer than rounded cells also supports this model [Goldmann et al., 1998]. The tension mediated by the actin stress fibers may not only establish cooperation between elongation of the leading edge and contraction of the posterior, but also regulate biochemical reactions in different regions of the cell. Furthermore, such mechanical effects may also be important to understand other living cooperative phenomena, such as proliferation and self-organization in an early embryo.

ACKNOWLEDGEMENTS

We thank Prof. E. Ito (Hokkaido Univ.) and Prof. T. Ushiki (Niigata Univ.) for their biological and technical advice. This work was supported in part by Special Funding for Basic Research from the Ministry of Education, Science, Sports, and Culture of Japan to K. K.

REFERENCES

Ashkin A, Dziedzic JM. 1989. Internal cell manipulation using infrared laser traps. Proc Natl Acad Sci USA 86:7914-7918.

Bausch AR, Ziemann F, Boulbitch AA, Jacobson K, Sackmann E. 1998. Local measurements of viscoelastic parameters of adherent cell surfaces by magnetic bead microrheometry. Biophys J 75:2038-2049.

Bausch AR, Moeller W, Sackmann E. 1999. measurement of local viscoelasticity and forces in living cells by magnetic tweezers. Biophys J 76:573-579.

Bereiter-Hahn J, Ilonka K, Lures H, Voth M. 1995. Mechanical basis of cell shape: investigations with the scanning acoustic microscope. Biochem Cell Biol 73:337-348.

Dembo M, Wang YL. 1999. Stresses at the Cell-to-Substrate Interface during Locomotion of Fibroblasts. Biophys J 76:2307-2316.

Evans E, Ritchie K, Merkel R. 1995. Sensitive force technique to probe molecular adhesion and structural linkages at biological interface. Biophys J 68:2580-2587.

Goldmann WH, Galneder R, Ludwig M, Kromm A, Ezzell RM. 1998. Differences in F9 and 5.51 cell elasticity determined by cell poking and atomic force microscopy. FEBS Lett 424:139-142

Haga H, Sasaki S, Kawabata K, Ito E, Ushiki T, Abe K, Sambongi T. 2000a. Elasticity mapping of living fibroblasts by AFM and immunofluorescence observation of cytoskeleton. Ultramicroscopy 82:253-258.

Haga H, Nagayama M, Kawabata K, Ito E, Ushiki T, Sambongi T. 2000b. Time-lapse viscoelastic imaging of living fibroblasts using force modulation mode in AFM. J Electron Microsc 49(3):473-481.

Henon S, Lenormand G, Richert A, Gallet F. 1999. A new determination of the shear modulus of the human erythrocyte membrane using optical tweezers. Biophys J 76:1145-1151.

Hildebrand JA, Rugar D. 1984. Measurement of cellular elastic properties by acoustic microscopy. J Microsc 134:245-260.

Horwitz AR, Parsons JT. 1999. Cell migration – movin' on. Science 286:1102-1103

Ingber DE. 1993. Cellular tensegrity: defining new rules of biological design that govern the cytoskeleton. J Cell Science 104: 613-627

Ingber DE. 1997. Tensegrity: the architectural basis of cellular mechanotransduction. Annu Rev Physiol 59:575-599

Kawabata K, Nagayama M, Haga H, Sambongi T. 2001. Mechanical effects on collective phenomena of biological systems: cell locomotion. Current Appl Phys 1:66-71

Lauffenburger DA, Horwitz AF. 1996. Cell migration; a physically integrated molecular process. Cell 84:359-369

Lures H, Hillmann K, Litniewski J, Bereiter-Hahn J. 1991. Acoustic microscopy of cultured cells: Distribution of forces and cytoskeletal elements. Cell Biophys 18:279-293.

Maciver SK, Wachssstock DH, Schwarz WH, Pollard TD. 1991. The Actin Filament Severing Protein Actophorin Promotes the Formation of Rigid Bundles of Actin Filaments Crosslinked with α-Actinin. J Cell Biol 115(6):1621-1628.

Peterson NO, McConnaughey WB, Elson EL. 1982. Dependence of locally measured cellular deformability on position on the cell, temperature and cytochalasin B. Proc Natl Acad Sci USA 79:5327-5331.

Radmacher M, Tillmann RW, Gaub HE. 1993. Imaging viscoelasticity by force modulation with the atomic force microscope. Biophys J 64:735-742.

Radmacher M, Fritz M, Kacher CM, Cleveland JP, Hansma PK. 1996. Measuring the Viscoelastic Properties of Human Platelets with the Atomic Force Microscope. Biophys J 70:556-567.

Rotsch C, Radmacher M. 2000. Drug-Induced Changes of Cytoskeletal Structure and Mechanics in Fibroblasts: An Atomic Force Microscopy Study. Biophys J 78:520-535.

Shao J, Hochmuth RM. 1996. Micropipette suction for measuring piconewton forces of adhesion and tether formation from neutrophil membranes. Biophys J 71:2892-2901.

Svoboba K, Schmidt CF, Branton D, Block SM. 1992. Conformation and elasticity of the isolated red blood cell membrane skeleton. Biophys J 63:784-793.

van Leeuwen FN, van Delft S, Kain HE, van der Kammen RA, Collard JG. 1999. Rac regulates phosphorylation of the myosin-Ⅱ heavy chain, actinomyosin disassembly and cell spreading. Nature Cell Biol 1:242-248.

Walch M, Ziegler U, Groscurth P. 2000. Effect of streptolysin O on the microelasticity of human platelets analyzed by atomic force microscopy. Ultramicroscopy 82:259-267.

Wang N, Stamenovic D. 2000. Contribution of intermediate filaments to cell stiffness, stiffening, and growth. Am. J Physiol Cell Physiol 279:C188-C194.

Wu HW, Kuhn T, Moy VT. 1998. Mechanical Properties of L929 Cells Measured by Atomic Force Microscopy: Effect of Anticytoskeletal Drugs and Membrane Crosslinking. Scanning 20:389-397.

Zaharak GI, McConnaughey WB, Elson EL. 1990. Determination of cellular mechanical properties by cell poking, with an application to leukocytes. J Biomech Eng 112:283-294.

Figure legends

FIGURE 1 Topographic (a), local stiffness (b), and viscous (c) images of a fibroblast (NIH3T3) obtained by the force modulation mode. All images are 80 μm square. The topographic image (a) is graphically shaded. In the stiffness image (b), increased brightness represents greater hardness. The elasticity of the cell is spatially inhomogeneous. Arrows indicate stress fibers covering the cellular surface and aligning along the direction of the cell crawling. In the viscous image (c), the brighter regions represent higher viscosity. The nuclear area within the oval appears to be less viscous than the periphery.

FIGURE 2 Time-lapse images of topography and local stiffness of a moving cell. All images are 80 μm square. Topographic and stiffness images measured simultaneously are shown as coupled images. The coupled images were taken every 10 minutes. The posterior portion of the cell body (marked rectangle in (a)) contracted, and a lamellipodia (marked rectangle in (d)) extended. The nucleus position (marked by a cross) moved downward. In

the images (a) and (b), the nucleus region (marked within an oval) is stiffer than the peripheral regions. Once the cell begins to move, the nucleus region becomes drastically softer.

FIGURE 3　Time-lapse images of topography and local stiffness of a staying cell. All images are 80 μm square. Images were taken at 10 min intervals. Topographic and stiffness images measured simultaneously are shown as coupled images. Neither the shape nor the stiffness of a cell changes over the 60 minute period.

FIGURE 4　Time dependence of the stiffness at the nucleus region of the moving (a) and the staying cells (b). The moving cell becomes softer with time, whereas the stiffness of the staying cell is almost constant.

Figure 1

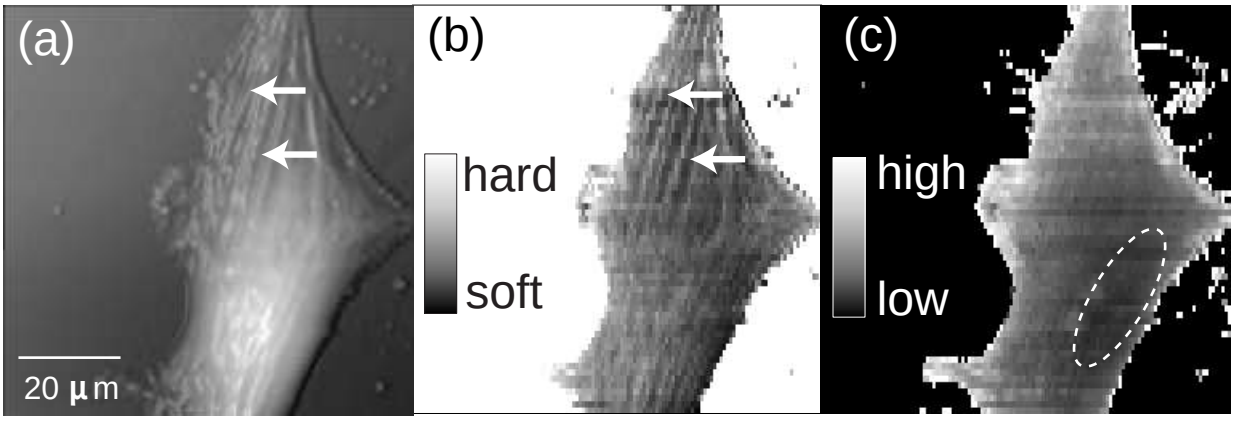

Figure 2

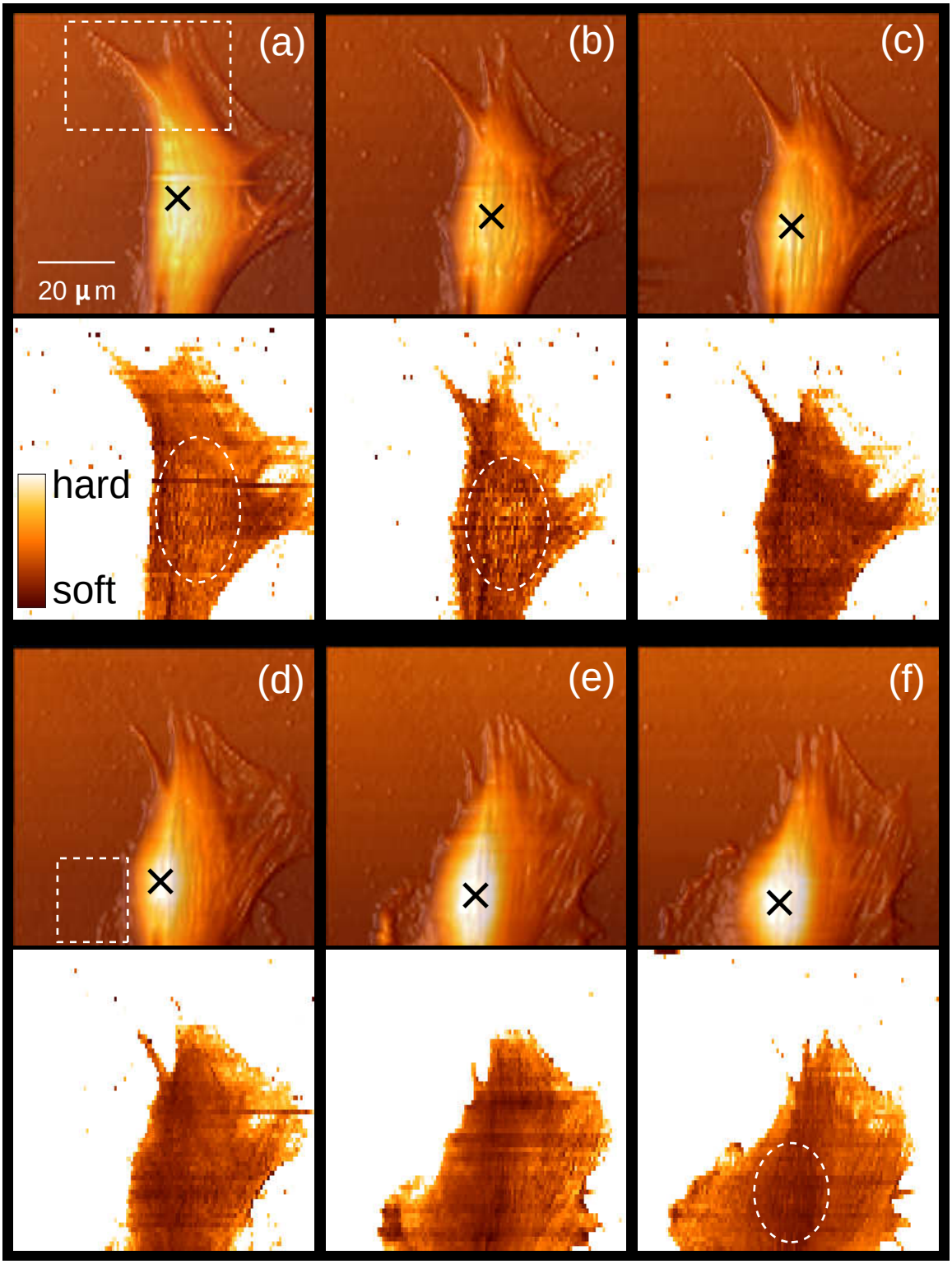

Figure 3

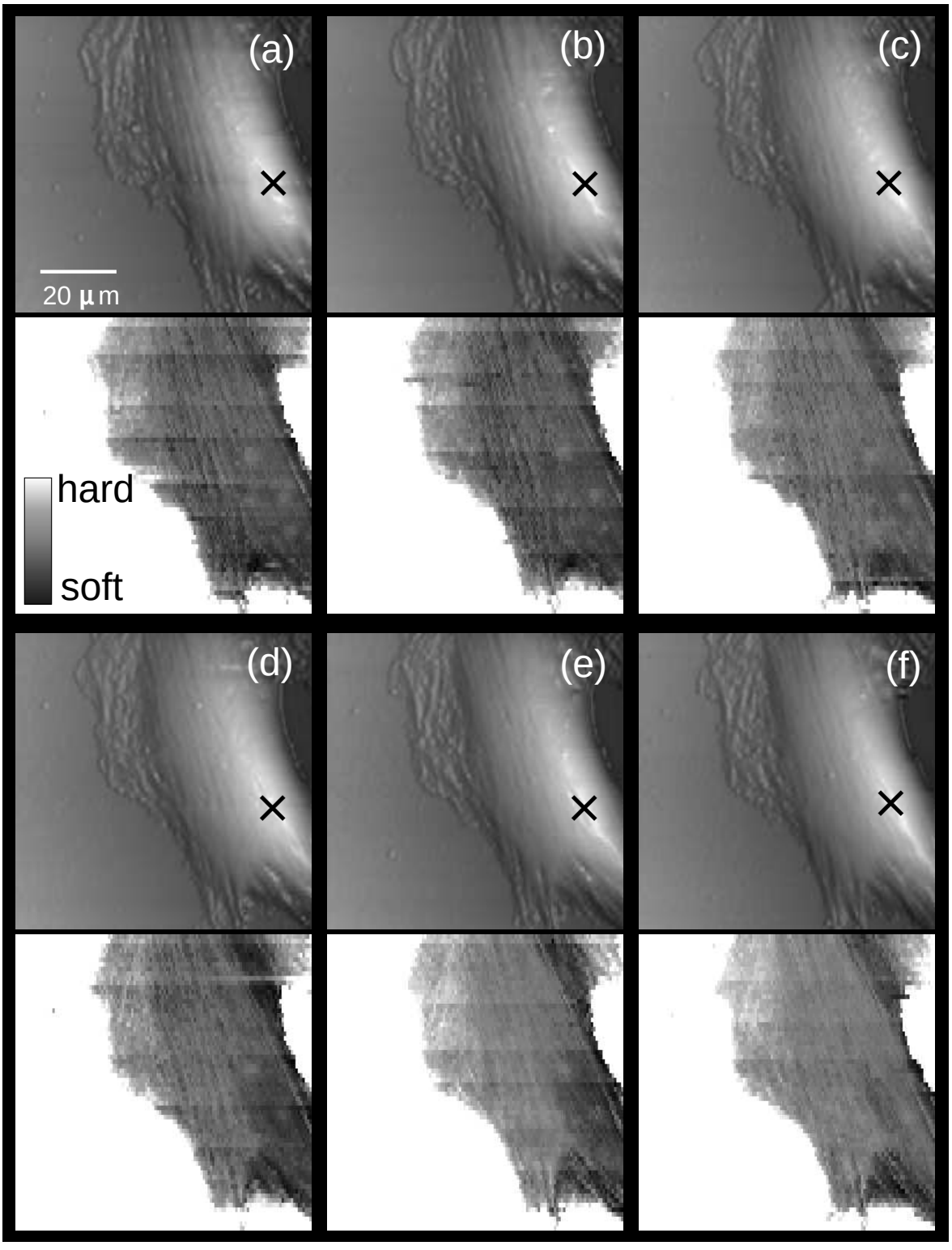

Figure 4

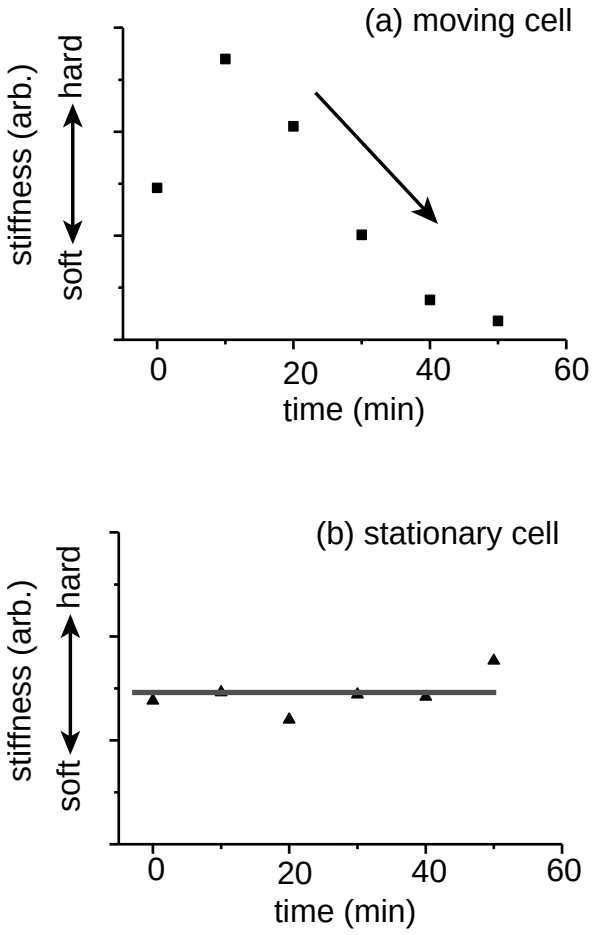
(a) moving cell
stiffness (arb.)
soft
hard
0
20
40
60
time (min)
(b) stationary cell
stiffness (arb.)
soft
hard
0
20
40
60
time (min)